The human thalamus is an integrative hub for functional brain networks

Kai Hwang, Maxwell Bertolero, William Liu, Mark D'Esposito

Helen Wills Neuroscience Institute and Department of Psychology, University of California Berkeley, CA, USA

KEY WORDS: Thalamus, Brain Networks, Graph Theory, Functional Connectivity, Diaschisis

Address correspondence to:

Kai Hwang Ph.D.

132 Barker Hall MC 3190

University of California Berkeley

California, CA 94720

USA

kai.hwang@berkeley.edu

Abstract

The thalamus is globally connected with distributed cortical regions, yet the functional significance of this extensive thalamocortical connectivity remains largely unknown. By performing graph-theoretic analyses on thalamocortical functional connectivity data collected from human participants, we found that the human thalamus displays network properties capable of integrating multimodal information across diverse cortical functional networks. From a meta-analysis of a large dataset of functional brain imaging experiments, we further found that the thalamus is involved in multiple cognitive functions. Finally, we found that focal thalamic lesions in humans have widespread distal effects, disrupting the modular organization of cortical functional networks. This converging evidence suggests that the human thalamus is a critical hub region that could integrate heteromodal information and maintain the modular structure of cortical functional networks.

Introduction

The cerebral cortex has extensive anatomical connections with the thalamus. Every cortical region receives projections from the thalamus, and in turn sends outputs to one or multiple thalamic nuclei (1). The thalamus is one of the most globally connected neural structures (2, 3); thalamocortical projections relay nearly all incoming information to the cortex, as well as mediate cortico-cortical communication (4). The mammalian brain can therefore be conceptualized as a thalamocortical system, thus full insight into brain function requires knowledge of the organization and properties of thalamocortical interactions.

The thalamus can be divided into two types of nuclei: first order and higher order thalamic nuclei (4-6). First order thalamic nuclei, such as the lateral geniculate nucleus (LGN), ventral posterior (VP) and ventral lateral (VL) nuclei, receive inputs from ascending sensory pathways or other subcortical brain regions. In contrast, higher-order thalamic nuclei, such as the mediodorsal (MD) and the pulvinar nuclei, receive inputs predominately from the cortex. More than half of the thalamus comprises higher order thalamic nuclei, which have both reciprocal and non-reciprocal connections with multiple cortical regions. These connectivity profiles suggest that in addition to relaying sensory and subcortical information to the cortex, another principle function of the thalamus is to mediate the transfer of information between cortical regions through cortico-thalamo-cortical pathways (5).

How a brain region such as thalamus processes and communicates information in functional brain networks can be inferred by its connectivity pattern (7). Graph-theoretic network analysis of resting-state functional MRI (rs-fMRI) data is well suited for exploring the network properties of the thalamocortical system (8). Functional connectivity analyses of rs-fMRI data

measures correlations of spontaneous fluctuations in blood oxygenation level dependent (BOLD) signals, which are not a direct proxy for anatomical connectivity but are largely constrained by anatomical connections (9, 10). Functional connectivity between two brain regions likely represents the phase-locking of the two regions' low-frequency oscillations of these two regions or coherent activity of high-frequency neuronal activity (11, 12).

Previous functional connectivity analyses of rs-MRI data have consistently revealed a modular organization structure of the human cerebral cortex, indicating that the cortex is composed of several specialized functional networks (13, 14). Each of these networks is potentially involved in executing a discrete set of cognitive functions relatively encapsulated from the other networks (15). Graph-theoretic measures can be used to quantify topographic properties of each brain region and make inferences on each region's network functions (16). For instance, a brain region with many within-network connections has a strong "provincial hub" property, presumably to promote within-network interactions for executing specialized functions of the network; whereas a brain region with many between-network connections has a strong "connector hub" property, presumably to mediate interactions between functional networks. Connector and provincial hubs have distinct contributions to modular organization. For example, a lesion study showed that damage to connector hubs, but not provincial hubs, causes more severe disruption of network's modular organization (17), suggesting that focal lesions to connector hubs can have a widespread impact on network organization when between-network connections are disrupted. Finally, cortical connector hubs are engaged by multiple cognitive tasks (18, 19), and exhibit increased activity when multiple functional networks are engaged by a behavioral task (15). These findings suggest that connector hubs are capable of multimodal and integrative processing through their extensive between-network connectivity (20).

The thalamus has been largely ignored in studies of brain network organization, and the topographic properties of the thalamocortical system within the large-scale organization of the human brain are largely unknown. Previous graph-theoretic studies of functional brain networks often exclude subcortical structures, or examine the thalamus with gross or no subdivisions. However, given its complex structure with multiple distinct nuclei, the thalamus is likely not uniformly interacting with the cortex. Different thalamic subdivisions have distinct structural connectivity with the cortex, and thus functional connectivity with the cortex (21-23). Traditionally, it is proposed that each thalamic subdivision functionally connects with cortical regions that belong to the same functional network for partially closed-loop, modality-selective processes (24). Based on this hypothesis, thalamic subdivisions should exhibit strong provincial hub (within-network) properties (Figure 1A). Alternatively, if a thalamic subdivision functionally interacts with cortical regions from multiple functional networks, this thalamic subdivision should exhibit strong connector hub (between-network) properties (Figure 1B). These hypotheses are not mutually exclusive—the thalamus could contain subdivisions that are involved in both modality-selective and multimodal, integrative processes.

The goal of this study was to elucidate the thalamus's network topological role in functional brain networks. To measure network properties of thalamocortical functional connectivity, we performed graph theoretic network analyses on rs-fMRI data collected from healthy human participants. To relate network topology to cognitive functions, we analyzed task-related activity of the thalamus using a meta-analysis of 10,449 functional neuroimaging experiments from the BrainMap database (19, 25). Finally, we examined the thalamus's contribution to cortical network organization by analyzing rs-fMRI data from human patients with focal thalamic lesions.

Results

Identification of Cortical Networks

To identify cortical functional networks, we first measured functional connectivity matrices between 333 cortical ROIs (26), then performed a network partition analysis to estimate cortical network organization (see Methods). Replicating previous studies (13-15, 26), we found that the cerebral cortex can be decomposed into 9 functional networks (Figure 2A).

Parcellation of the Thalamus

Given that the thalamus can be subdivided using different approaches, we performed our analyses using three different atlases based on data from rs-fMRI, diffusion tensor imaging (DTI), and postmortem histology (Figure 2 A-C; see Methods for details). Using RS-fcMRI data, we identified thalamic subdivisions that demonstrated the strongest functional connectivity with the different cortical functional networks reported above (Figure 2A; henceforth referred to as the functional parcellation atlas). We further replicated these results with an independent dataset, and found high correspondence between datasets (normalized mutual information = 0.64, z-scored Rand coefficient =144.13, $p < 1.0e-05$). The Oxford-FSL thalamocortical structural connectivity atlas (Figure 2B) subdivides the thalamus based on structural connectivity (estimated using probabilistic diffusion tractography on DTI data) to seven large cortical areas: primary motor, primary somatosensory, occipital, premotor, prefrontal (including medial and

orbitofrontal cortices), parietal, and temporal cortices (23). The Morel atlas (Figure 2C) subdivides the thalamus into smaller nuclei based on cyto- and myelo-architecture information from five postmortem brains (27, 28). We further classified each thalamic nucleus from the Morel atlas into first order or higher order thalamic nuclei (4, 5) .

Network Properties of Thalamocortical Functional Connectivity

To determine each thalamic subdivision's network property, we estimated functional connectivity between each thalamic voxel and every cortical ROI (see Methods) to generate a thalamocortical network graph. Graph metrics were calculated for every thalamic voxel, and averaged across voxels for each the two categories of thalamic nuclei (first order and higher order). For comparison, the same graph metrics were calculated for each cortical ROI by only considering cortico-cortical functional connectivity.

Provincial Hub Property Analyses. Provincial hub property can be measured by within module degree (WMD), a z-scored measure of the number of within-network connections each region has (29). Higher values reflect more within-network connections. We found that both first order and higher order thalamic nuclei exhibited high WMD values that were comparable to cortical regions defined as cortical provincial hubs (Figure 3A; cortical provincial hubs mean WMD = 1.15, SD = 0.26; first order thalamic nuclei mean WMD = 1.27, SD = 1.79, higher order thalamic nuclei mean WMD = 1.64, SD = 1.92; cortical provincial hubs defined as cortical ROIs

with WMD values greater than 90% of all cortical ROIs, threshold = 0.8; see Supplementary Figure 1 for locations of cortical provincial hubs).

Connector Hub Property Analyses. Connector hub property can be measured by participation coefficient (PC), which is a measure of the strength of inter-network connectivity for each region normalized by their expected value (29). Higher values reflect more inter-network connections. We found that both first order and higher order thalamic nuclei exhibited high PC values that were comparable to cortical connector hubs (Figure 3B cortical connector hubs mean PC = 0.69, SD = 0.06; first order thalamic nuclei mean PC = 0.74, SD = 0.13, higher order thalamic nuclei mean PC = 0.77, SD = 0.11; cortical connector hubs defined as cortical ROIs with PC values greater than 90% of all cortical ROIs, threshold = 0.61; see Supplementary Figure 1 for locations of cortical connector hubs. Note that here connector hubs are defined as regions that exhibit high PC values, and could contain regions with both high and low WMD values).

Spatial Distribution of Connector and Provincial Hub Properties in the Thalamus. High PC and WMD values were found throughout the thalamus (Figure 4A-B). To determine differences in the spatial distribution of connector and provincial hub properties in the thalamus, we identified thalamic voxels that exhibited WMD or PC values greater than cortical connector and provincial hubs. We found that anterior, medial, posterior, and dorsal parts of the thalamus exhibited both strong provincial and connector hub properties, whereas portions of the lateral thalamus also exhibited strong connector hub property (Figure 4C). A small portion of the anterior thalamus has only strong provincial hub property.

Connector and Provincial Hub Properties of Each Thalamic Subdivision. We calculated the median WMD and PC values across voxels for each thalamic subdivision, and compared those values to cortical connector and provincial hubs. Based on the functional parcellation atlas, thalamic subdivisions that showed dominant functional coupling with cingulo opercular (CO), default mode (DM), frontoparietal (FP), medial temporal (mT), and superior frontoparietal (sFP) networks exhibited high WMD values numerically comparable to cortical provincial hubs (Fig 5A). Based on the Oxford-FSL thalamocortical structural connectivity atlas, thalamic subdivisions with dominant structural connectivity with the prefrontal cortex and temporal cortices showed high WMD values comparable to cortical provincial hubs (Figure 5B). Based on the Morel histology atlas, thalamic subdivisions with high WMD values comparable to cortical provincial hubs included the anterior nucleus (AN), LGN, VL, intralaminar nuclei (IL), lateral posterior nucleus (LP), MD, medial pulvinar (PuM), and ventral anterior nucleus (VA) nucleus (Figure 5C). For connector hub properties, we found that all thalamic subdivisions exhibited high PC values comparable or higher than cortical connector hubs (Figure 5D-F).

Replication of results. We replicated the WMD and PC analyses using an independent rs-fMRI dataset; the spatial correlation values across both cortical ROIs and thalamic voxels between the test and replication datasets for PC and WMD scores were 0.74 (degrees of freedom = 2558, $p < 1.0e-05$) and 0.78 (degrees of freedom = 2558, $p < 1.0e-05$), respectively. We also replicated our results using a different cortical ROI definition template that consists of 320 cortical ROIs (30), the thalamic voxel-wise spatial correlation values for PC and WMD scores

were 0.63 (degrees of freedom = 2225, $p < 1.0e-05$) and 0.78 (degrees of freedom = 2225, $p < 1.0e-05$), respectively.

Connectivity Patterns of Specific Thalamic Nuclei. Based on the Morel histology atlas, we found that AN, LGN, VL, IL, LP, MD, PuM, and VA exhibited both strong provincial and connector hub properties comparable to cortical hubs. To further probe their connectivity patterns, for each nucleus we calculated their mean functional connectivity strength with each of the 9 cortical functional networks (using partial correlations, see Methods), and divided by the nucleus's summated total connectivity strength with all networks. If a nucleus is diffusely interacting with all functional networks, then it should devote ~11% (1/9 = 0.11) of its total connectivity for each network. In contrast, if a nucleus only interacts with a selective network, the majority of its connectivity strength should be devoted to that network, while connectivity with other networks should be considerably lower. We found that each of these thalamic nuclei exhibited a diffuse functional connectivity pattern, with strong connectivity (>11% of its total connectivity strength) with multiple cortical functional networks (Figure 6).

Meta-Analysis of the BrainMap Database

We found that multiple thalamic subdivisions exhibited both strong provincial and connector hub properties, suggesting that the thalamus is capable of mediating information communication between multiple functional brain networks, each of which is putatively associated with a distinct set of cognitive functions (15). We tested the hypothesis that the

thalamus is involved in multiple cognitive functions by analyzing results from a published meta-analysis of 10,449 functional neuroimaging studies (19). This published meta-analysis derived latent variables—an ontology of cognitive functions or "cognitive components"—that best described the relationship between 83 behavioral tasks and corresponding brain activity. From this data, a "cognitive flexibility score" can be estimated by summing the number of cognitive components that are engaged by every brain region (19). If the thalamus is an integrative connector hub, it should exhibit a high cognitive flexibility score reflecting that it is recruited by multiple cognitive components.

Consistent with it's role as a connector hub, the thalamus was found to be involved in multiple cognitive components (Figure 7A). Previous studies have found that cortical connector hubs also exhibit a high cognitive flexibility score (15, 19). Both first order and higher order nuclei exhibited higher cognitive flexibility scores when compared to cortical connector hubs (first order nuclei mean = 4.13, higher order nuclei mean = 3.43, cortical connector hubs mean = 1.78; randomized permutation tests $p < 1.0e-04$). We further examined the specific cognitive components (C1-C12, see ref 19 for details) that recruited each of the thalamic subdivisions. As an example, VL, with projections to motor and premotor cortices (24), is recruited by components C1 and C2 that predominately recruit motor cortices (Figure 7B). However, VL also participates in other cognitive components that recruit lateral prefrontal, medial prefrontal, and parietal cortices (C8, C9, C12, Figure 7B).

Thalamic lesions have Global and Distal Effects on Cortical Network Organization

Whole-brain modularity can be measured by Newman's modularity Q (31), a comparison between the number of connections within a module to the number of connections between modules. Modularity quantifies the ability of the brain to differentiate into separable sub-networks and is an essential property found in many complex systems (32). If thalamic subdivisions serve as connector hubs for functional brain networks, lesions to those subdivisions should reduce brain modularity (as measured by Q). While on average all thalamic subdivisions showed high PC values, there is spatial variation of voxel-wise PC values within the thalamus (Figure 4B). Therefore, the scale of reduction in modularity should correlate with the degree of lesioned thalamic voxels' mean PC value. In three patients with focal and unilateral thalamic lesions (Figure 8A), the difference in modularity between the lesioned hemisphere versus the intact hemisphere was calculated, and converted to a z-score by normalizing to the hemispheric difference in modularity calculated from all healthy subjects from the test dataset (mean hemispheric difference in Q for healthy subjects = 0.008, SD = 0.048). We focused on interpreting interaction effects (lesioned versus intact hemispheric difference) to control for non-specific effects not caused by the lesion. In all three patients, modularity was lower in the lesioned hemisphere (Figure 8B). Patients with higher PC values in the damaged thalamic nuclei exhibited a greater reduction in modularity (Figure 8C). We did not find a relationship between the size of the lesion, WMD values (Figure 8D), and changes in modularity.

A reduction in modularity following a thalamic lesion suggests a disruption in cortical network organization. To test this hypothesis, we compared each patient's brain network organization against the network organization derived from healthy subjects by calculating the

normalized mutual information (NMI) of each patient's functional network composition against the composition in healthy subjects (Figure 2A). NMI evaluates the similarity of network composition between patients and healthy controls, which NMI = 1 suggests perfect correspondence between network partition results. For comparison, we also calculated NMI values for each healthy control from an independent replication dataset (see methods for detail). We found that thalamic lesions distorted the organization and composition of cortical functional networks, as indicated by lower NMI values for the patients (patients: mean = 0.33, *SD* = 0.17; controls from replication dataset: mean = 0.57, *SD* = 0.19; randomized permutation test $p < 0.01$).

Discussion

In this study, we provide evidence suggesting that the human thalamus is a critical integrative hub for functional brain networks. First, we found that the thalamus has strong between-network connectivity with multiple cortical functional networks. From a meta-analysis of 10,449 neuroimaging experiments, we further found that the thalamus is engaged by multiple cognitive functions, supporting a role in multimodal information processing. Finally, we found that focal thalamic lesions cause a disruption of the modular structure of cortical functional networks, further underscoring the critical contribution of thalamic function to brain network organization.

The human brain is composed of modular functional networks (15), which comprise provincial hubs — brain regions important for within network communication — and connector hubs — brain regions important for communication between networks. Here, we used graph-theoretic measures to estimate provincial and connector hub properties of the thalamus. Consistent with traditional interpretations of thalamic function, multiple thalamic subdivisions exhibited strong provincial hub properties. However, all thalamic subdivisions also displayed strong connector hub properties, suggesting that similar to cortical connector hubs, the thalamus has strong functional connectivity with multiple functional networks. Cortical connector hubs play a hypothetical role of integrating information across segregated functional brain networks (15, 18-20). The thalamus's widespread connectivity pattern allows the thalamus to send and access information across diverse cortical functional networks. Via convergence of information, the thalamus may serve as an integrative hub that subserves multiple cognitive functions. Although it has previously been proposed that the thalamus is more than just a relay station (5),

serving to mediate cortical to cortical communication within a network, the notion that the thalamus also plays integrative role interacting with multiple functional brain networks has received less attention in studies of thalamic function.

Higher order thalamic nuclei, which receive inputs predominately from the cortex, are hypothesized to provide trans-thalamic routes to support cortico-cortical interactions within a functional network that receive its projections (5, 33). For example, the posterior nucleus transfers information from primary area to secondary somatosensory areas (34). Likewise, the pulvinar has extensive reciprocal connections with striate and extrastiate visual cortices (35), and is thought to modulate information communication between visual areas (33, 36). In contrast, first order thalamic nuclei, which receive projections from peripheral sensory organs or other subcortical structures, have projections to primary cortices, and are thought to act as modality-selective relays to relay a limited type of afferent signal to the cortex. Our graph-theoretic analyses of thalamocortical functional connectivity provide novel evidence suggesting that both first order and higher order thalamic nuclei not only participate in information exchange between cortical regions that they project to, but also further interact with multiple cortical functional networks.

Thalamic nuclei project to and receive projections from multiple brain regions that belong to different functional brain networks. For example, higher order nuclei have higher concentration of "matrix" thalamocortical cells that show diffuse thalamocortical projections unconstrained by the boundaries of cortical topographic representations, and receive non-reciprocal cortico-thalamic innervations from multiple cortical regions (1, 37). The inhibitory thalamic reticular nucleus, rich in GABAergic cells, also receives input from the cortex and the basal ganglia, and further modulate activity in both first order and higher order thalamic nuclei

(4). Thalamic nuclei could also have dense reciprocal connections with cortical connector hubs that in turn are connected with multiple cortical functional networks. These results suggest that thalamocortical functional connectivity has an anatomical substrate capable of simultaneously receiving and transmitting signals between multiple cortical functional networks.

Consistent with its role as a connector hub, we found that the thalamus is one of the most "cognitively flexible" brain regions, indicating that the thalamus is involved in a diverse range of behavioral tasks. This observation from the meta-analysis of the BrainMap database is further supported by several representative empirical studies demonstrating that the thalamus mediates interactions between higher order cognitive processes (e.g., attention and working memory) and more elementary sensorimotor functions (33, 38, 39). For example, a non-human primate electrophysiology study found that deactivating the pulvinar reduced the attentional effects on sensory-driven evoked responses recorded in V4 (39). Also, optogenetically perturbing thalamic activity in rodents impaired animals' ability to select between conflicting visual and auditory stimuli (40). Finally, VL lesions in humans impair their ability to utilize a memorized cue in working memory to guide visual search of multiple visual stimuli (38). Together, results from our graph analyses of thalamocortical functional connectivity and meta-analysis of thalamic task-related activity patterns suggest that the thalamus participates in interactions between multiple functional cortical networks, networks that are putatively involved in distinct cognitive functions.

Previous studies suggest that connector hubs are critical for maintaining the modular architecture of functional brain networks. For example, in humans, connector hubs are more active when more functional networks are engaged in a task (15), and focal damage to connector hubs decreases whole brain modularity (17). In addition, disruption of connector hub function

with transcranial magnetic stimulation increases between-network connectivity (41), which will in turn decrease modularity. We found that in patients with focal thalamic lesions, the lesioned hemisphere's modularity was lower when compared to the intact hemisphere. Thus, the effect of a thalamic lesion is not constrained only to those cortical regions it directly projects to. Instead, we found that a focal thalamic lesion causes "connectomal diaschisis" (42) in cortical functional networks, affecting distributed cortical regions and large-scale connectivity patterns. Further, the scale of reduction in whole-brain modularity correlated with the degree of a lesioned thalamic subdivision's connector hub property. Thus, our lesion analysis suggests that in addition to functional integration, the thalamus is important for maintaining the modular structure of functional brain networks.

Methods

Datasets

For the main analyses, we analyzed publically available resting-state fMRI (rs-fMRI) data from 303 subjects (mean age = 21.7, STD = 2.87, age range =19-27, 131 males) that were acquired as part of the Brain Genomics Superstruct dataset (43). For each subject, two runs (6.2 minutes each) of rs-fMRI data were collected using a gradient-echo echo-planar imaging sequence with the following parameters: relaxation time (TR) = 3000 ms, echo time (TE) = 30 ms, flip angle = 85 degrees, 3 mm^3 isotropic voxels with 47 axial slices. Structural data were acquired using a multi-echo T1-weighted magnetization-prepared gradient-echo (MPRAGE) sequence (TR = 2,200 ms, TE= 1.54 ms for image 1 to 7.01 ms for image 4, flip angle = 7 degree, 1.2 mm^3 isotropic voxel). We replicated our main analyses with publically available rs-fMRI data from 62 healthy adults (mean age = 22.59, SD = 2.45, age range =19-27, 26 males) that were acquired as part of the NKI-Rockland sample (44). For each subject, 9 minutes and 35 seconds of rs-fMRI data were acquired using a multiband gradient-echo echo-planar imaging sequence (TR = 1400 ms, echo time = 30 ms, multiband factor = 4, flip angle = 65 degrees, 2 mm^3 isotropic voxels with 64 axial slices). Structural data were acquired using a MPRAGE (TR = 1900 ms, TE= 2.51 ms, flip angle = 9 degree, 1 mm^3 isotropic voxel). For both datasets, subjects were instructed to stay awake and keep their eyes open.

For the lesion analyses, we analyzed rs-fMRI data from three patients with focal thalamic lesions (ages: S1 = 83 years, S2 = 49 years, S3 = 55 years, all males, all were scanned at least 6 months after their stroke). Two runs of rs-fMRI data were collected (10 minutes each; TR = 2000

ms, echo time = 30 ms, flip angle = 72 degrees, 3.5 mm^2 in plane resolution with 34 axial 4.2 mm slices). Structural images were acquired using a MPRAGE sequence (TR = 2,300 msec, TE = 2.98 msec, flip angle = 9°, 1 mm^3 voxels). Patients were instructed to stay awake and keep their eyes open. Informed consent was obtained from all patients in accordance with procedures approved by the Committees for Protection of Human Subjects at the University of California, Berkeley.

Functional MRI Data Preprocessing

Image preprocessing was performed the software Configurable Pipeline for the Analysis of Connectomics (45). First brain images were segmented into white matter (WM), gray matter, and cerebral spinal fluid (CSF). Rigid body motion correction was then performed to align each volume to a temporally averaged volume, and a boundary-based registration algorithm was used to register the EPI volumes to the anatomical image. Advanced Normalization Tools (ANTS) was used to register the images to MNI152 template using a nonlinear normalization procedure (46). We then performed nuisance regression to further reduce non-neural noise and artifacts. To reduce motion-related artifacts, we used the Friston-24 regressors model during nuisance regression (47). WM and CSF signals were regressed using the CompCor approach with five components (48). Linear and quadratic drifts were also removed. The physical proximity between the thalamus and the ventricles could result in blurring of fMRI signal. We regressed out the mean signal from CSF, WM, and gray matter that were within 5 voxels (10 mm) from the thalamus. Data were bandpass filtered from 0.009–0.08 Hz. Finally, signal intensity was scaled to a whole-brain mode value of 1000. No spatial smoothing was performed.

Identifying Cortical Functional Networks

Following preprocessing, mean rs-fMRI time-series were extracted from 333 cortical ROIs (26), and concatenated across runs for subjects with multiple rs-fMRI scans. Cortico-cortical functional connectivity was assessed in each subject by computing Pearson correlations between all pairs of cortical ROIs, resulting in a 333 x 333 correlation matrix. This correlation matrix was then thresholded at different thresholds to retain the strongest percentages of functional connections. For each subject, putative cortical functional networks were then identified using a recursive InfoMap algorithm to partition the matrix into modules by integrating results across thresholds (15). We then aggregated individual subjects' module organization by creating a consensus matrix (a value of 1 where the two ROI are in the same module and a value of 0 elsewhere) for each subject. The average of these consensus matrices across subjects was then submitted to the same recursive InfoMap algorithm to identify group-level cortical functional networks (49). Networks with 5 or fewer ROIs were eliminated from further analyses, and no networks were assigned to those ROIs.

Thalamus Parcellation

To localize the thalamus, the Morel Atlas (28) was used to define its spatial extent (2227 2 mm^3 voxels included in the atlas). To identify thalamic subdivisions, three different thalamic atlases were utilized. We first performed a custom winner take all functional parcellation using rs-fMRI data by calculating partial correlations between the mean BOLD signal for each cortical

functional network identified and the signal in each thalamic voxel, partialing out signal variance from other functional networks. Partial correlations were then averaged across subjects, and each thalamic voxel was labeled according to the cortical network with the highest correlations. The Morel atlas identified thalamic nuclei based on cyto- and myelo-architecture in stained slices of post-mortem tissue collected from five postmortem brains (27), and further transformed to MNI space (28). The Oxford-FSL thalamic structural connectivity atlas defined thalamic subdivisions based on its structural connectivity with different cortical regions estimated from diffusion imaging data (23).

Thalamic and Cortical Nodal Properties

To formally quantify the network properties of thalamocortical functional connectivity, for each subject, we calculated the partial correlation between each thalamic voxel's preprocessed BOLD signal and the mean BOLD signal of each cortical ROI, while partialing out signal variance from all other cortical ROIs. Given the large number of cortical ROIs, a dimension reduction procedure using principal component analysis was performed on signals from cortical ROIs not included in the partial correlation calculation, and eigenvectors that explained 95% of variance were entered as additional nuisance regressors in the model. We chose partial correlations over full correlations because past studies have shown detailed thalamocortical connectivity patterns could be obscured without accounting for shared variance between cortical regions (50). Note that no correlations were calculated between thalamic voxels. We also quantified network properties of cortical ROIs by calculating its Pearson correlation with all other cortical ROIs. Correlation matrices were thresholded by density and submitted to

further graph analyses. All graph metrics were calculated across a range of thresholds that retain top 1% to top 10% strongest percentages of functional connections, and averaged across thresholds.

For each thalamic voxel and cortical ROI, we then calculated participation coefficient (PC) and within module degree (WMD) (29). PC value for each thalamic voxel or cortical ROI *i* is defined as:

$$PC = 1 - \sum_{s=1}^{N_M} \left(\frac{K_{is}}{K_i}\right)^2$$

where K_i is the sum of connectivity weight of *i* and K_{is} is the sum of connectivity weight between *i* and cortical network *s*. If a region has connections uniformly distributed to all cortical networks, then its PC value will be close to 1; on the other hand, if its connectivity is concentrated within a specific cortical network, its PC value will be close to 0. We further divided PC values by its theoretical upper limit based on the number of functional networks, so that the highest possible PC value given the network architecture would be 1.

To calculate WMD, correlation matrices were first binarized by setting weights above the cost threshold to 1. Weights were binarized to equate the connectivity weights between thalamocortical and cortico-cortical networks. WMD is calculated as

$$WMD = \frac{K_i - \overline{CW_s}}{\sigma CW_s}$$

Where $\overline{CW_s}$ is the average number of connections between all cortical ROIs within cortical network *s,* and σCW_s is the standard deviation of the number of connections of all ROIs in network *s*. K_i is the number of connections between *i* and all cortical ROIs in network *s*. Because our goal was to understand the thalamus's contribution to cortical network organization, thalamic

voxels' WMD scores were calculated using the mean and standard deviation of within-network degree (number of intra-network connections) for each cortical functional network.

For all patients, rs-fMRI volumes with framewise displacement (FD) that exceeded 0.5 mm were removed from further analysis (scrubbed) after band-pass filtering (mean percentage of frames scrubbed for patients = 13.34%, SD = 9.32%). Lesion masks were manually traced in the native space according to visible damage on a T1-weighted anatomical scan, and further guided by hyperintensities on a T2-weighted FLAIR image. Lesion masks were then warped into the MNI space using the same non-linear registration parameters calculated during preprocessing.

Meta-Analysis of Functional Neuroimaging Experiments in the BrainMap Database

We reanalyzed data presented in a previously published meta-analysis of the BrainMap database (19). In the meta-analysis, a hierarchical Bayesian model was used to derive a set of 12 cognitive components that best describe the relationship between behavioral tasks and patterns of brain activity in the BrainMap database (25). Specifically, each behavioral task (e.g., Stroop, stop-signal task, finger tapping) engages multiple cognitive components, and in turn each cognitive component is supported by a distributed set of brain regions. To determine whether or not a thalamic voxel is recruited by a cognitive component, a threshold of p = 1e-5 was used. This is an arbitrary yet stringent threshold that was used in two prior studies (15, 19). Critically, there is potential spatial overlap between components. Therefore, brain regions that can flexibly participate in multiple cognitive components could be identified by calculating the number of cognitive components each brain region engages. The number of cognitive components was summed for each voxel and cortical ROIs and defined as a "cognitive flexibility" score (19).

References

1. Jones EG (2001) The thalamic matrix and thalamocortical synchrony. *Trends Neurosci*. 24(10):595-601.
2. Cole MW, Pathak S, & Schneider W (2010) Identifying the brain's most globally connected regions. *Neuroimage* 49(4):3132-3148.
3. Crossley NA, *et al*. (2013) Cognitive relevance of the community structure of the human brain functional coactivation network. *Proc Natl Acad Sci U S A* 110(28):11583-11588.
4. Sherman SM & Guillery RW (2013) *Functional connections of cortical areas : A new view from the thalamus* (MIT Press, Cambridge, Mass.).
5. Sherman SM (2016) Thalamus plays a central role in ongoing cortical functioning. *Nat Neurosci* 16(4):533-541.
6. Guillery RW & Sherman SM (2002) Thalamic relay functions and their role in corticocortical communication: Generalizations from the visual system. *Neuron* 33(2):163-175.
7. Passingham RE, Stephan KE, & Kotter R (2002) The anatomical basis of functional localization in the cortex. *Nature Reviews Neuroscience* 3(8):606-616.
8. Bullmore E & Sporns O (2009) Complex brain networks: Graph theoretical analysis of structural and functional systems. *Nature Reviews Neuroscience* 10(3):186-198.
9. Honey CJ, *et al*. (2009) Predicting human resting-state functional connectivity from structural connectivity. *Proceedings of the National Academy of the United States of America* 106(6):2035-2040.

10. Hermundstad AM, *et al*. (2013) Structural foundations of resting-state and task-based functional connectivity in the human brain. *Proc Natl Acad Sci U S A* 110(15):6169-6174.

11. Wang L, Saalmann YB, Pinsk MA, Arcaro MJ, & Kastner S (2012) Electrophysiological low-frequency coherence and cross-frequency coupling contribute to BOLD connectivity. *Neuron* 76(5):1010-1020.

12. Scholvinck ML, Maier A, Ye FQ, Duyn JH, & Leopold DA (2010) Neural basis of global resting-state fMRI activity. *Proc Natl Acad Sci U S A* 107(22):10238-10243.

13. Yeo BT, *et al*. (2011) The organization of the human cerebral cortex estimated by intrinsic functional connectivity. *J. Neurophysiol*. 106(3):1125-1165.

14. Power JD, *et al*. (2011) Functional network organization of the human brain. *Neuron* 72(4):665-678.

15. Bertolero MA, Yeo BT, & D'Esposito M (2015) The modular and integrative functional architecture of the human brain. *Proc Natl Acad Sci U S A* 112(49):E6798-6807.

16. Sporns O, Honey CJ, & Kötter R (2007) Identification and classification of hubs in brain networks. *PLoS ONE* 2(10):e1049.

17. Gratton C, Nomura EM, Perez F, & D'Esposito M (2012) Focal brain lesions to critical locations cause widespread disruption of the modular organization of the brain. *J Cogn Neurosci* 24(6):1275-1285.

18. Cole MW, *et al*. (2013) Multi-task connectivity reveals flexible hubs for adaptive task control. *Nat Neurosci* 16(9):1348-1355.

19. Yeo BT, *et al*. (2016) Functional Specialization and Flexibility in Human Association Cortex. *Cereb. Cortex* 26(1):465.

20. van den Heuvel MP & Sporns O (2013) An anatomical substrate for integration among functional networks in human cortex. *J Neurosci* 33(36):14489-14500.

21. Yuan R, *et al*. (2015) Functional topography of the thalamocortical system in human. *Brain structure & function*.

22. Arcaro MJ, Pinsk MA, & Kastner S (2015) The Anatomical and Functional Organization of the Human Visual Pulvinar. *J Neurosci* 35(27):9848-9871.

23. Behrens TE, *et al*. (2003) Non-invasive mapping of connections between human thalamus and cortex using diffusion imaging. *Nat Neurosci* 6(7):750-757.

24. Alexander GE, DeLong MR, & Strick PL (1986) Parallel organization of functionally segregated circuits linking basal ganglia and cortex. *Annual Review of Neuroscience* 9:357-381.

25. Laird AR, Lancaster JL, & Fox PT (2005) BrainMap - The social evolution of a human brain mapping database. *Neuroinformatics* 3(1):65-77.

26. Gordon EM, *et al*. (2016) Generation and evaluation of a cortical area parcellation from resting-state correlations. *Cereb. Cortex* 26(1):288-303.

27. Morel A, Magnin M, & Jeanmonod D (1997) Multiarchitectonic and stereotactic atlas of the human thalamus. *J Comp Neurol* 387(4):588-630.

28. Krauth A, *et al*. (2010) A mean three-dimensional atlas of the human thalamus: generation from multiple histological data. *Neuroimage* 49(3):2053-2062.

29. Guimera R & Nunes Amaral LA (2005) Functional cartography of complex metabolic networks. *Nature* 433(7028):895-900.

30. Craddock RC, James GA, Holtzheimer PE, 3rd, Hu XP, & Mayberg HS (2012) A whole brain fMRI atlas generated via spatially constrained spectral clustering. *Hum Brain Mapp* 33(8):1914-1928.

31. Newman ME (2006) Modularity and community structure in networks. *Proc Natl Acad Sci U S A* 103(23):8577-8582.

32. Sporns O & Betzel RF (2016) Modular Brain Networks. *Annu. Rev. Psychol.* 67:613-640.

33. Saalmann YB, Pinsk MA, Wang L, Li X, & Kastner S (2012) The pulvinar regulates information transmission between cortical areas based on attention demands. *Science* 337(6095):753-756.

34. Theyel BB, Llano DA, & Sherman M (2010) The corticothalamocortical circuit drives higher-order cortex in the mouse. *Nature Neuroscience* 13(1):84-U246.

35. Adams MM, Hof PR, Gattass R, Webster MJ, & Ungerleider LG (2000) Visual cortical projections and chemoarchitecture of macaque monkey pulvinar. *J Comp Neurol* 419(3):377-393.

36. Saalmann YB & Kastner S (2011) Cognitive and perceptual functions of the visual thalamus. *Neuron* 71(2):209-223.

37. McFarland NR & Haber SN (2002) Thalamic relay nuclei of the basal ganglia form both reciprocal and nonreciprocal cortical connections, linking multiple frontal cortical areas. *J. Neurosci.* 22(18):8117-8132.

38. de Bourbon-Teles J, *et al.* (2014) Thalamic Control of Human Attention Driven by Memory and Learning. *Curr. Biol.* 24(9):993-999.

39. Zhou H, Schafer RJ, & Desimone R (2016) Pulvinar-Cortex Interactions in Vision and Attention. *Neuron* 89(1):209-220.

40. Wimmer RD, *et al*. (2015) Thalamic control of sensory selection in divided attention. *Nature* 526(7575):705-709.

41. Gratton C, Lee TG, Nomura EM, & D'Esposito M (2013) The effect of theta-burst TMS on cognitive control networks measured with resting state fMRI. *Frontiers in systems neuroscience* 7:124.

42. Carrera E & Tononi G (2014) Diaschisis: past, present, future. *Brain* 137(Pt 9):2408-2422.

43. Holmes AJ, *et al*. (2015) Brain genomics superstruct project initial data release with structural, functional, and behavioral measures. *Scientific data* 2:150031.

44. Nooner KB, *et al*. (2012) The NKI-Rockland sample: A model for accelerating the pace of discovery science in psychiatry. *Front Neurosci* 6:152.

45. Sikka S, *et al*. (2014) Towards automated analysis of connectomes: The configurable pipeline for the analysis of connectomes (c-pac). *5th INCF Congress of Neuroinformatics, Munich, Germany*.

46. Avants BB, Epstein CL, Grossman M, & Gee JC (2008) Symmetric diffeomorphic image registration with cross-correlation: Evaluating automated labeling of elderly and neurodegenerative brain. *Med. Image Anal.* 12(1):26-41.

47. Friston KJ, Williams S, Howard R, Frackowiak RS, & Turner R (1996) Movement-related effects in fmri time-series. *Magn. Reson. Med.* 35(3):346-355.

48. Behzadi Y, Restom K, Liau J, & Liu TT (2007) A component based noise correction method (CompCor) for bold and perfusion based fmri. *Neuroimage* 37(1):90-101.

49. Lancichinetti A & Fortunato S (2012) Consensus clustering in complex networks. *Scientific reports* 2:336.

50. Zhang D, *et al*. (2008) Intrinsic functional relations between human cerebral cortex and thalamus. *J Neurophysiol* 100(4):1740-1748.

Figures

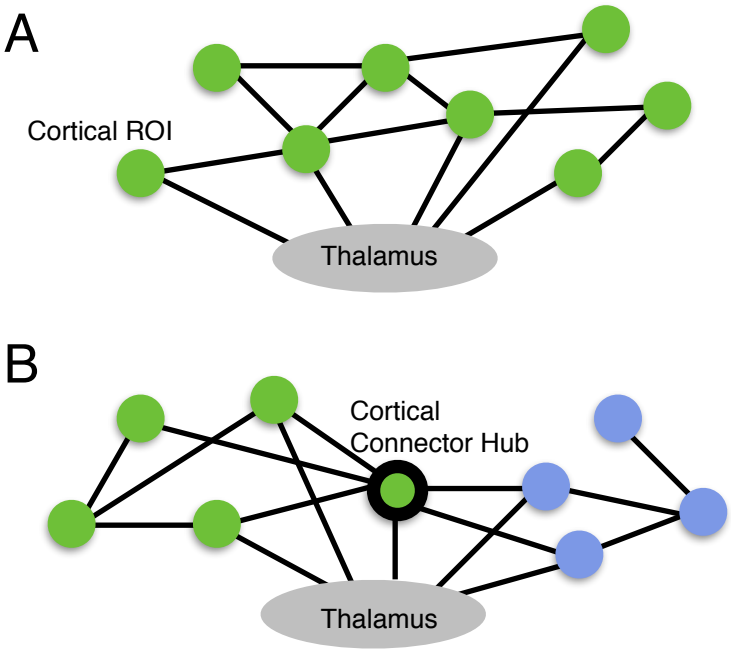

Figure 1. (A) As a provincial hub, the thalamus is connected with cortical regions that belong to the same cortical functional network (represented in solid green circles). (B) As a connector hub, the thalamus is connected with cortical regions in multiple cortical functional networks (one network colored in green and the other in cyan).

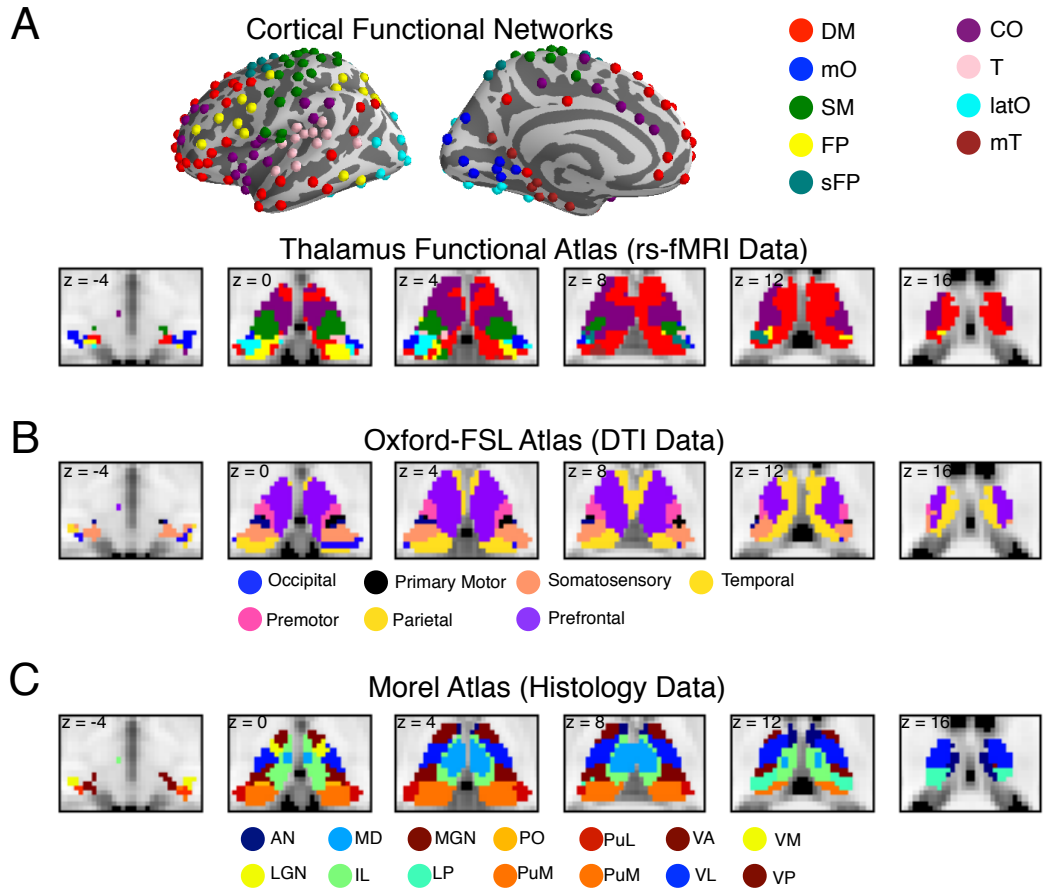

Figure 2. (A) Cortical functional networks and thalamic parcellation derived from functional connectivity analyses between the thalamus and each cortical network using rs-fMRI data. Network abbreviations (based on its most predominant location): default mode (DM), medial occipital (mO), somato-motor (SM), fronto-parietal (FP), superior fronto-parietal (sFP), cingulo-opercular (CO), temporal (T), lateral occipital (latO), medial temporal (mT). A detailed list of the specific ROIs for each network are provided in Supplementary Table 1. (B) Structural connectivity based segmentation of the thalamus using the Oxford-FSL atlas. Each thalamic subdivision was labeled based on the cortical region it is most structurally connected with. (C) Histology based thalamic parcellation using the Morel atlas. Abbreviations for thalamic nuclei: anterior nucleus (AN), intralaminar (IL), lateral posterior (LP), lateral geniculate nucleus (LGN), medial geniculate nucleus (MGN), medial dorsal (MD), medial pulvinar (PuM), inferior pulvinar (PuI), lateral pulvinar (PuL), anterior pulvinar (PuA), posterior (Po) nuclei, ventral posterior (VP), ventral anterior (VA), ventral medial (VM), Ventral lateral (VL).

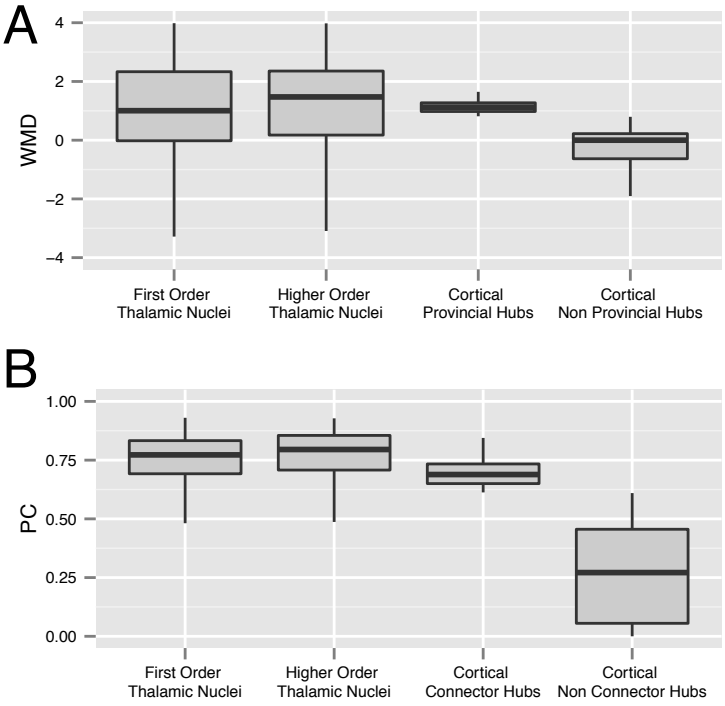

Figure 3. (A) Box plots of WMD values summarized by categories of thalamic nuclei and cortical ROIs. Categories of thalamic nuclei defined based on (4, 5). Cortical connector and provincial hubs are cortical ROIs that have high PC or WMD values (greater than 90% of all cortical ROIs), other ROIs are defined as non-hub regions. (B) Box plots of PC values summarized by categories of thalamic nuclei and cortical ROIs. First order thalamic nuclei included AN, LGN, MGN, VL, and VP. Higher order thalamic nuclei included IL, MD, LP, Po, Pulvinar, VA, and VM. Box plot percentiles (5^{th} and 95^{th} for outer whiskers, 25^{th} and 75^{th} for box edges) calculated across voxels for each thalamic nuclei type or across cortical ROIs for each cortical ROI type.

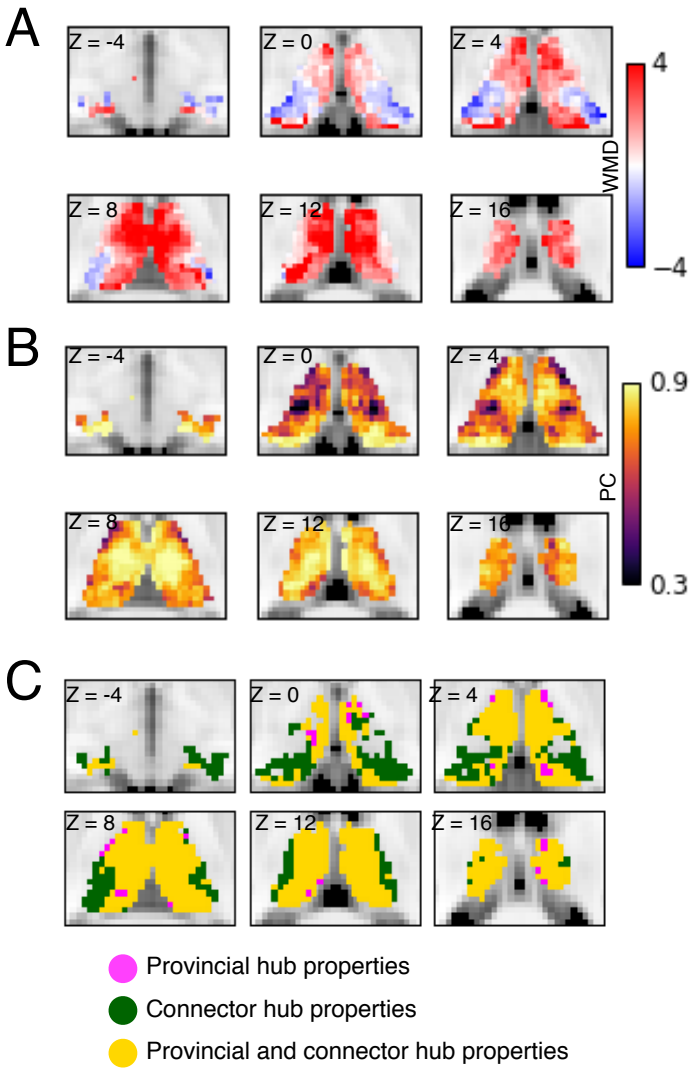

Figure 4. (A) WMD and (B) PC values of thalamic voxels. (C) Location of voxels with strong connector (colored in pink), provincial (colored in green), or connector plus provincial hub properties (colored in gold) in the thalamus. Only thalamic voxels that exhibited PC and/or WMD values greater than 90% of all cortical ROIs are displayed.

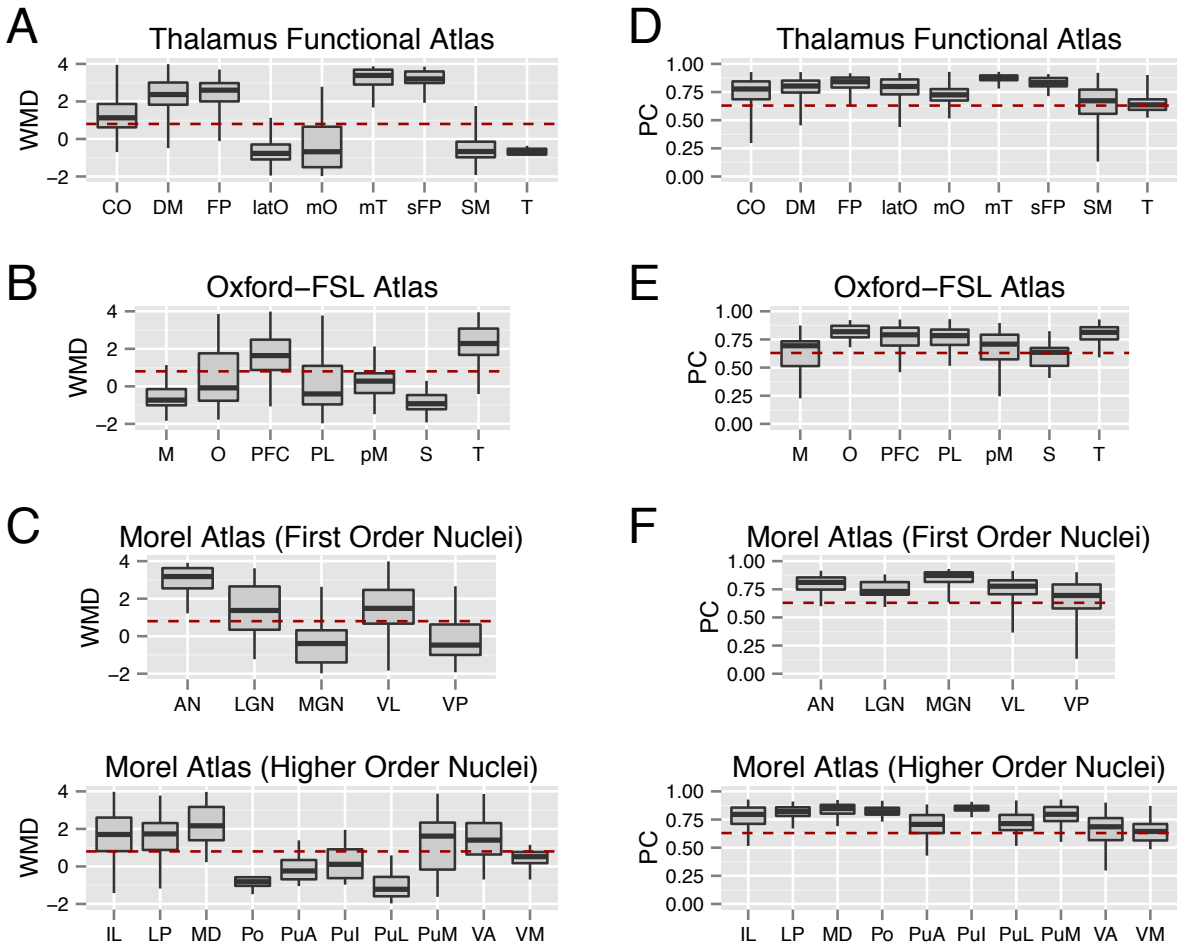

Figure 5. (A-C) Box plots of WMD values (A-C) and PC values (D-F) for all thalamic voxels for each thalamic atlas. The dashed line represents minimal WMD or PC values of cortical provincial or connector hubs. Abbreviations for the Oxford-FSL atlas: motor (M), occipital (O), prefrontal (PFC), parietal (PL), premotor (pM), somatosensory (S), temporal (T). Box plot percentiles (5th and 95th for outer whiskers, 25th and 75th for box edges) calculated across voxels for each thalamic subdivision.

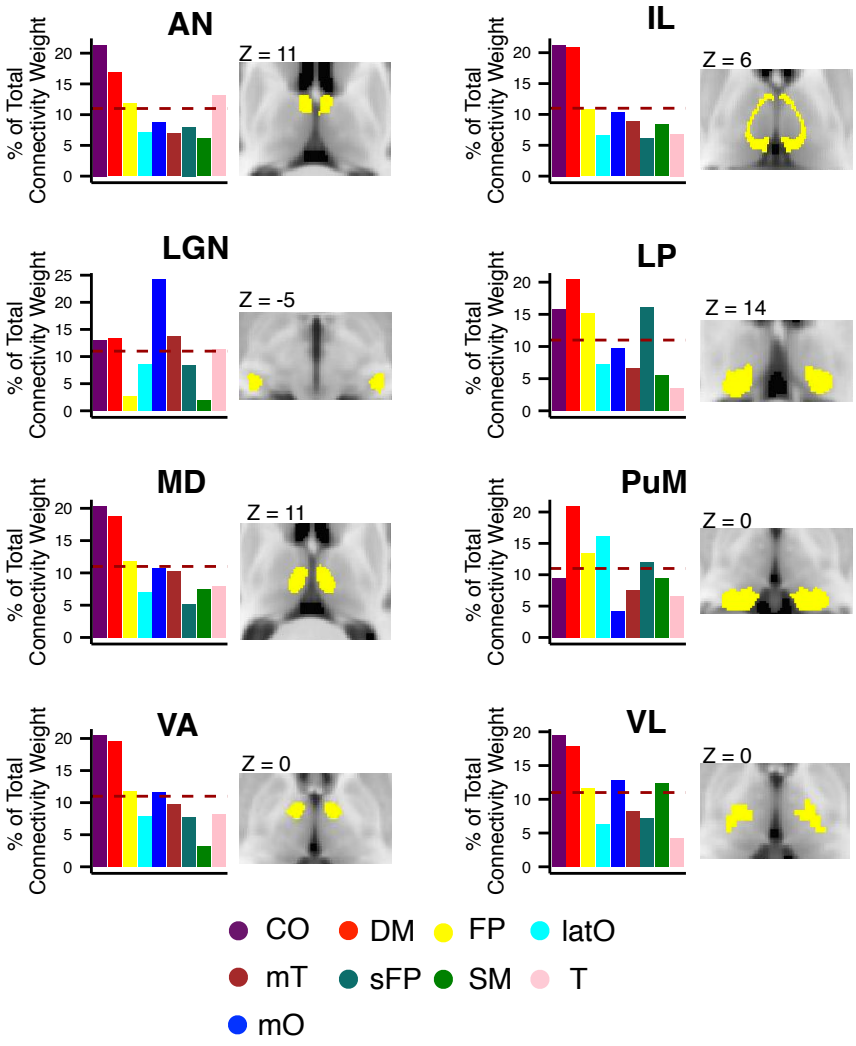

Figure 6. Cortical functional networks most strongly connected with the following thalamic nuclei: AN, LGN, VL, VA, VM, IL, LP, MD, PuM. Thalamic nuclei (labeled in yellow) are displayed on axial MRI images. The bar graphs represent the distribution of connectivity strength between thalamic nuclei and each of the 9 cortical functional networks. The dashed line represents the expected proportion of total connectivity if connections were equally distributed across networks.

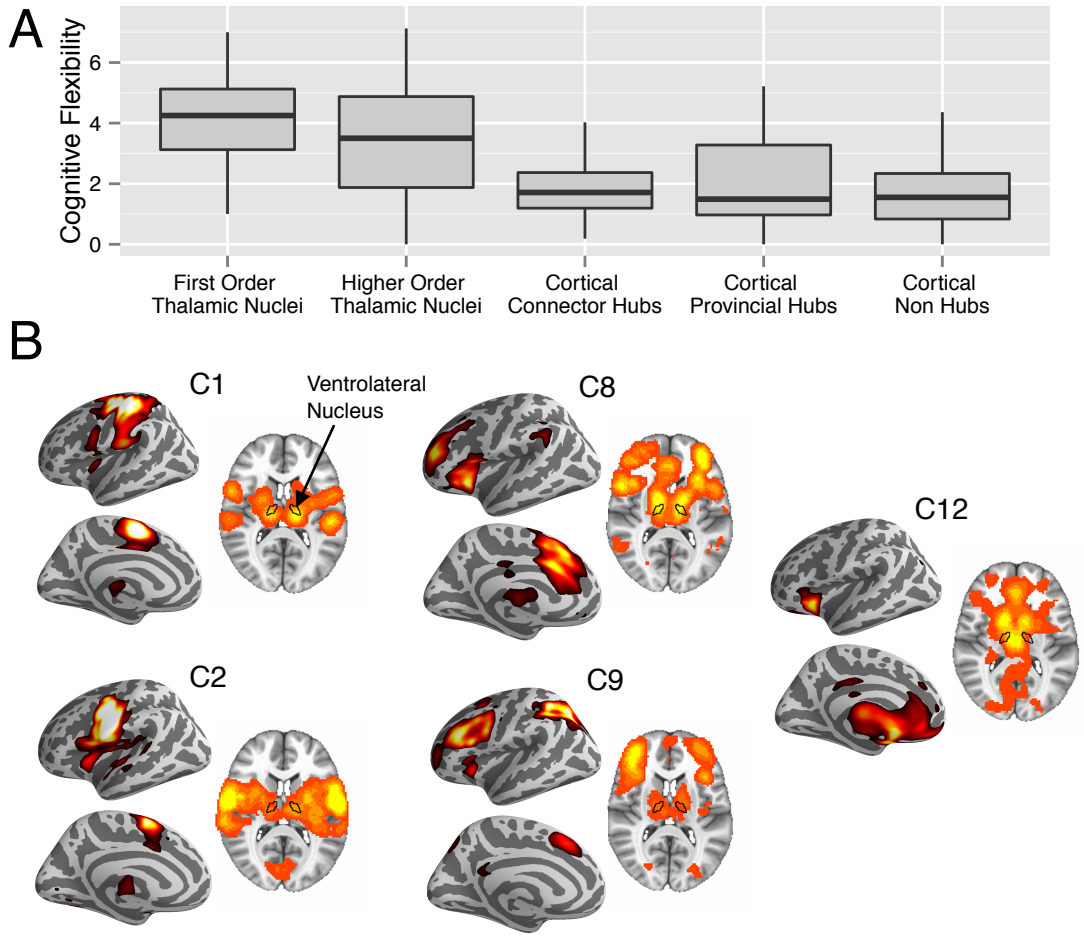

Figure 7. (A) Box plot of cognitive flexibility scores (number of cognitive components) summarized by categories of thalamic nuclei and cortical ROIs. Box plot percentiles (5^{th} and 95^{th} for outer whiskers, 25^{th} and 75^{th} for box edges) calculated across voxels for each thalamic nuclei type or across cortical ROIs for each cortical ROI type. (B) Spatial distribution of brain activity engaged by each cognitive components recruited by the thalamic nucleus VL.

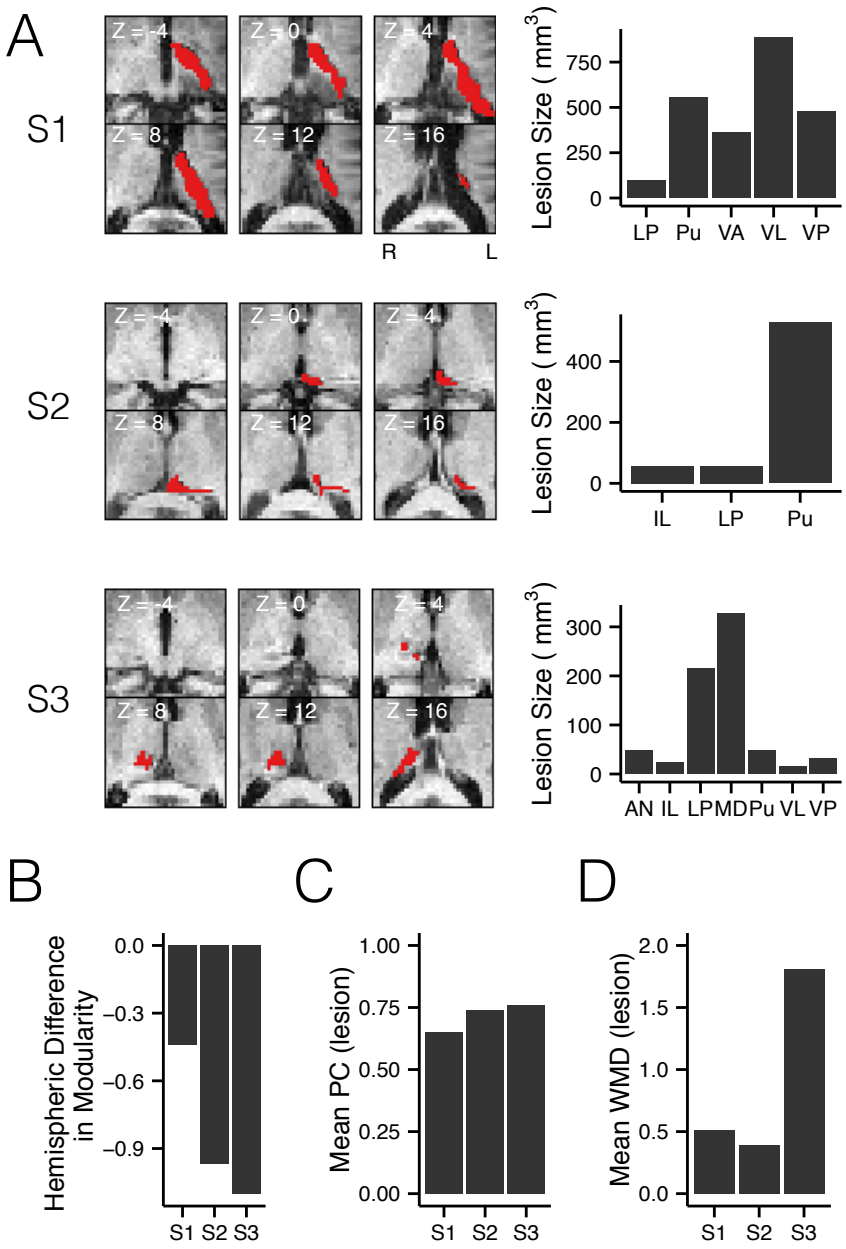

Figure 8. (A). MRI scans of thalamic lesions (marked in red) in three patients (S1-S3). Lesion size for each patient in each thalamic subdivision is summarized in bar graphs. (B) Individual patient's Z-scores of hemispheric differences in modularity score. (C) Individual patient's mean PC value of lesioned voxels. (D) Individual patient's mean WMD value of lesioned voxels.

Acknowledgements

This work was supported by NIH Grants RO1 NS79698 and F32 NS090757. The Morel atlas was obtained by a written consent with Professor G. Szekely from the Computer Vision Laboratory of ETH Zurich, Switzerland. This project was made possible by a collaborative agreement allowing comprehensive access to the BrainMap database, a copyrighted electronic compilation owned by the University of Texas Board of Regents. BrainMap is supported by National Institutes of Health, National Institute of Mental Health Award R01 MH074457.